ELSEVIER

Journal of Atmospheric and Solar-Terrestrial Physics 67 (2005) 1827–1836

Journal of ATMOSPHERIC AND SOLAR-TERRESTRIAL PHYSICS

www.elsevier.com/locate/jastp

Wavelet analysis applied to magnetograms: Singularity detections related to geomagnetic storms

Odim Mendes Jr.[a,*], Margarete Oliveira Domingues[b], Aracy Mendes da Costa[a], Alícia L. Clúa de Gonzalez[a]

[a]*National Institute for Space Research - INPE/CEA/DGE, 12245-970 São José dos Campos, São Paulo, Brazil*
[b]*National Institute for Space Research - INPE/CTE/LAC, 12245-970 São José dos Campos, São Paulo, Brazil*

Available online 25 August 2005

Abstract

When the interplanetary magnetic field carried by the solar wind opposes to the Earth intrinsic magnetic field, a substantial transfer of energy into the terrestrial magnetosphere takes place. If this condition persists for several hours, the magnetosphere becomes very disturbed. As a result, at mid-to-low latitudes a ring current starts to develop and at high latitudes ionospheric currents (electrojet and field-aligned currents) dominate. The ring current provides the geomagnetic conditions for magnetic storms to settle down. Wavelet analysis is becoming an usual tool since they allow the decomposition of data, functions or operators into different frequency or scale components. Accordingly, wavelet transforms seem to be suited to analyze short-lived high-frequency phenomena such as discontinuities (*shocks*) in signals and transient structures. In this work, the remarkable ability of wavelets to highlight the singularities associated with discontinuities present in the horizontal component of the Earth's magnetic field is explored. Magnetograms obtained at five magnetic stations for two geomagnetic storms have been analyzed by a Daubechies orthogonal wavelet transform. The wavelet coefficient magnitudes at three levels have been studied. In both cases, the physical discontinuities in the horizontal component of the geomagnetic field are clearly detected by means of these coefficients identifying the disturbed interval related to geomagnetic storms. Wavelet analysis has proved to be a useful tool in the identification of the geomagnetic storms using non-processed data.

Keywords: Wavelet analysis; Multi-resolution analysis; Geomagnetic storm; Sun–Earth coupling; Planetary electrodynamics

1. Introduction

Under suitable geometric and energetic conditions, a disturbed solar wind plasma flowing out from the Sun can reach the Earth environment. When the interplanetary magnetic field (IMF) carried by the solar wind opposes the Earth's intrinsic magnetic field, a substantial transfer of energy into the terrestrial magnetosphere occurs. If this condition persists for several hours, the magnetosphere becomes very disturbed (Gonzalez et al., 1994; Clúa de Gonzalez et al., 2004). As a consequence of an enhanced level of solar wind–magnetosphere coupling, the normally existing magnetospheric and ionospheric quiet currents are widened and intensified (Jankovicová et al., 2002). If magnetic effects are considered, the ring current dominates at middle and low latitudes and a system of ionospheric electrojet currents flowing in the auroral oval dominates at higher latitudes. These current systems characterize magnetic

*Corresponding author.
E-mail address: margarete@lac.inpe.br (O. Mendes Jr.).

1364-6826/$ - see front matter © 2005 Elsevier Ltd. All rights reserved.
doi:10.1016/j.jastp.2005.07.004

disturbance phenomena that are called, geomagnetic storms and geomagnetic substorms respectively, (Kamide et al., 1998). Another current system provides a link between the high- and the low-latitude currents: the field-aligned currents, which contribute to increase the complexity of these current systems. The presence of currents in the boundary and tail of the magnetosphere and the ionosphere also produce magnetic disturbances. All these current systems affect especially the horizontal component of the geomagnetic field at the Earth surface. This component is used in the calculation of the *Dst* index, that accounts for the variations in the equatorial ring current (Sugiura and Kamei, 1991), and the *AE* index, that describes the disturbances in the auroral electrojet current system (Mayaud, 1980).

When hot ions are injected into the inner magnetosphere, the geometry of the geomagnetic field causes them to drift around the Earth, forming a westward ring current (O'Brien and McPherron, 2000). This current is composed of linear and nonlinear processes from the dawn-dusk electric field. Although the injection of particles and its magnetic effect may be approximated as a linear process, the trapping mechanism and consequently the resultant ring current intensity may not be approximated as a linear process, since it depends on the history of the cross tail potential difference. This effect will limit the efficiency of the linear prediction filter of the ring current from the solar wind parameters (Takahashi et al., 1990). Forecasting the state of the ring current is a necessity to forecast the magnetic field in the magnetosphere. The magnetic field variation produced by the ring current decreases the magnetic field at the Earth's surface and this depression is measured by the *Dst* index (Sugiura and Kamei, 1991). The *Dst* index represents the longest commonly used measure of the state of the ring current and therefore it is essential in such forecasting (Baker, 1998).

A typical storm includes a substantial ring current that develops over a few hours and then recovers over several days (Kamide et al., 1998). Geomagnetic disturbances observed at mid-to-low latitudes show less spatial irregularities than those observed at high latitudes, because theses regions are far away from the origins of disturbance and they are not directly linked to the IMF. The magnetic variations at low latitude, ordinarily used to derive the *Dst* index, are regarded as representing the whole magnetospheric process without severe locality. Even so, the magnetic disturbances at middle and low latitudes exhibit a rather complicated time and/or spatial variation.

The magnetic field measured at mid-to-low latitudes can be affected significantly by variations of the solar wind ram pressure, which produces changes in the magnetopause current. This process gives place to a storm sudden commencement (SSC), when an increase in the horizontal magnetic field is observed at mid-to-low latitudes. It is generally considered that the solar wind ram pressure represents only a linear correction to the magnetometer measurements. This contribution can be dynamical in nature and spatially dependent, since the compression of the magnetopause can affect the magnetometer locations with different strengths (Valdivia et al., 1999). On the other hand, the degree of relative contribution of the ionospheric current to the magnetospheric current systems observed in magnetograms may be an important feature that can be examined through the characteristics of the SSC (Tsunomura, 1998).

In order to study such phenomena, the wavelet technique has been choosen because of its ability to analyze non-stationary signals. Wavelet analysis is becoming a widespread tool since it allows the decomposition of data, functions, or operators into different frequency or scale components (Strang and Nguyen, 1996; Foufoula-Georgiou and Kumar, 1995; Daubechies, 1992; Ruskai et al., 1992; Chui, 1992a, b). Each component can then be studied with a resolution that matches its scale, i.e. at high frequencies the wavelet is very narrow, while at low frequencies it is broad. As a result, wavelet transforms are good tools to "zoom in" on short-lived high-frequency phenomena, such as singularities in signal and transient structures. As each scale of the wavelet transform is associated with a frequency band, the wavelet transform decomposition levels represent the frequency bands detected in the geomagnetic storms. In a particular scale, because of the wavelet analysis properties, the wavelet coefficients will have small amplitudes (Meyer, 1990) where the magnetic field is *smooth*. On the other hand, they will have larger amplitudes where singularities and transient structures occur in the magnetograms. Some applications to geomagnetic field data have been reported by Bayer et al. (2001) and in the references therein.

In order to detect the variations of the horizontal component of the geomagnetic field related to geomagnetic storms, singularities have been analyzed by means of the wavelet technique. The purpose of this work is to present an alternative way to identify quiescent from non-quiescent periods related to geomagnetic storms using magnetograms instead of the processed *Dst* index.

2. Wavelet technique applied to singularity detections

The wavelet transform is a linear transform with the property of being covariant under translation and dilatation. It can be used in the analysis of non-stationary signals to obtain information on the frequency variations of these signals and to detect their structures localization in time and/or in space. The time/space localization occurs because the wavelet function ψ is defined in a finite interval. In a general way, wavelets have time–frequency localization, with the

time resolution, t, inversely proportional to the frequency resolution, ξ, such that

$$\Delta t \times \Delta\xi = constant,$$

as illustrated by Fig. 1. The upper panel of this figure shows a diagram of the time–frequency plane ($t \times \xi$ plane). In the lower panel a zoom out scheme of a wavelet function dilatation in this plane is shown for three different j-levels. It can be seen from this time–frequency plane that as the levels (scales) increase, the time resolution decreases. In this figure, we can also observe that there is a relationship between the scale j and the frequency range or the pseudo-frequency, denoted by $\bar{\xi}_j$. Abry has derived this frequency in Hz, as

$$\bar{\xi}_j = \frac{\xi_\psi}{j\Delta t},$$

where Δt is the sampling rate, ξ_ψ is the central frequency of the wavelet ψ in Hz (Abry, 1997, pp. 11–12). It is also possible to define a pseudo-period as the inverse of the pseudo-frequency. To calculate ξ_ψ, it is necessary to associate it with the chosen wavelet, a purely periodic signal of a certain frequency in order to maximize the fast Fourier transform (FFT) of the wavelet modulus. The central frequency-based approximation captures the main wavelet oscillations. Then, this frequency is a convenient and simple characterization of the leading dominant frequency of the wavelet. Fig. 2 shows a plot of a wavelet function and the corresponding periodic signal used to calculate ξ_ψ.

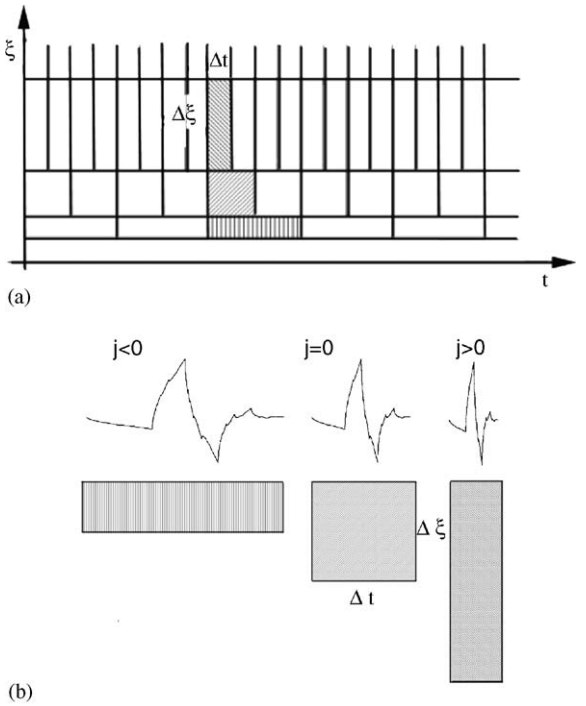

Fig. 1. (a) Shows the time–frequency plane ($t \times \xi$ plane) and (b) shows a zoom-out scheme of wavelet function dilatation in this plane for three different j-levels.

In wavelet analysis, signals $f(t)$ are represented by series like

$$f(t) = \sum_{j=-\infty}^{\infty} \sum_{k=-\infty}^{\infty} d_k^j \psi_k^j(t),$$

where $\psi_k^j(t) = \psi(2^j t - k)$ are called mother wavelet (Daubechies, 1992; Chui, 1992b). The wavelet coefficients d_k^j are expressed by

$$d_k^j = 2^j \int_{\infty}^{-\infty} f(t)\psi(2^\ell t - k)\,\mathrm{d}t.$$

In a multi-level basis, wavelet coefficients are also known as "details" because they can be seen as the difference between the signal in two consecutive scale levels. Actually, the wavelet transform is a map of the signal to its wavelet coefficients. As has been proved the amplitudes of the wavelet coefficients are directly proportional to the local smoothness and to the local norm of the function it represents (Meyer, 1990).

It is possible to build up wavelet functions using a mathematical tool known as multi-resolution analysis (Mallat, 1991; Daubechies, 1992; Jawerth and Sweldens, 1994). The Daubechies orthogonal wavelet functions are examples of this type of construction. As they form an orthogonal system, no redundant information is stored. Those functions do not have analytical expressions and are not symmetric. For the purposes of this work, the Daubechies orthogonal order two wavelet (shown in Fig. 2) has been chosen because:

(a) this wavelet family is slightly asymmetric, thus a *future time* information is used to calculate the wavelet coefficients;

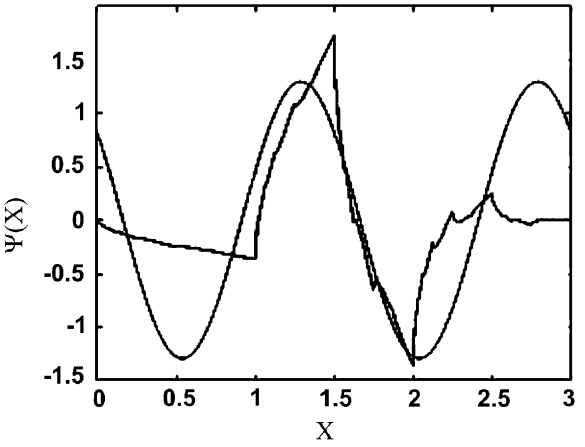

Fig. 2. Example of the Daubechies orthogonal order two wavelet and the corresponding frequency-based approximation, for which $\xi_\psi = 0.66667$ (calculated using Wavelet tool box, Matlab).

(b) this wavelet family is adequate to detect shock-like singularities, because it uses few coefficients and it is a good representation of low-order polynomials.

A more detailed description of the wavelet technique applied to atmospheric signals can be found in Domingues et al. (2005).

The methodology to process the magnetograms was based on the following steps:

(1) To calculate the discrete wavelet transform of the magnetograms.
(2) To analyze the wavelet coefficients of the decomposition levels.
(3) To choose the wavelet coefficient thresholds that allow the singularity detection in the magnetic disturbance associated with the geomagnetic storms. In the characterization of a geomagnetic disturbance, all the squared wavelet coefficients greater than the chosen threshold are considered.

In this analysis, the threshold has been defined as the minimum value of the square coefficients that exceeds the local background fluctuations. Then, a new time series was constructed using the inverse discrete wavelet transform, that sets to zero the other wavelet coefficients not associated with the geomagnetic disturbance. The reconstructed and the original series were then compared to determine the amount of energy lost, considering the L^2 norm. This procedure has established the threshold criterium for all magnetograms analyzed in this work: the reconstructed series must contain more than 99% of the signal restored energy. Then, the position of the largest amplitude-remained wavelet coefficients after the threshold cut-off process indicates the *shock candidate regions*.

The essential feature of wavelets used in this work is their ability to highlight the singularities associated with *shocks* (discontinuities) present in a total horizontal component (H) or in the North–South component (X) of the Earth's magnetic field. This property was applied to geomagnetic field signals, recorded by magnetograms, associated with geomagnetic storms and quiet periods.

3. Datasets

To illustrate the singularity detection related to geomagnetic storms using the wavelet analysis, two geomagnetic storms were selected. This work is restricted to the analysis of magnetograms obtained at middle-to-low latitudes only, because we are mostly interested in the development of the ring current system related to the geomagnetic storm behavior.

These events occurred near the solar maximum period (solar cycle 21). The selected time intervals include the geomagnetic disturbance and a previous period of relatively low geomagnetic activity. The first geomagnetic storm, discussed in details by Mendes et al. (1994), started on November 7, 1978 at 22:27 UT and corresponds to a moderate magnetic storm with a maximum $Dst = -47$ nT at 02:00 UT on November 8. The second one started on August 29, 1979 with a minimum $Dst = -140$ nT at 19:00 UT and corresponds to an intense magnetic storm, discussed in details by Tsurutani et al. (1988).

In order to develop this analysis, 1 min time resolution magnetograms obtained at five magnetic stations were used. These datasets have been downloaded from WDC (2004) and SPIDR (2004). A six-day interval of the geomagnetic field components H or X was considered as the dataset.

The geographic and geomagnetic coordinates and magnetic local time (MLT)[1] of these magnetic stations are given in Table 1. The magnetic stations Kakioka, Hermanus and Boulder are located at medium and low latitudes and are longitudinally worldwide spaced. For these latitudes, the total horizontal intensity H and the North–South component X can be used indiscriminatedly, and usually only one of them is available for each station in the data centers.

The auroral stations Fort Churchil and Dumont d'Urville located in the north and south hemispheres, respectively, have been included as guidelines to check the storm behavior at higher latitudes.

It is important to mention that in the derivation of the standard *Dst* index, in the 1978–1979 period, only four magnetic stations were used: Honolulu, Kakioka, Hermanus and San Juan (Iyemori et al., 1998). Boulder was included in this study, because the data from Honolulu and San Juan were not available at WDC (2004), for the selected periods.

Fig. 3 shows the magnetograms obtained at Fort Churchill, Boulder, Kakioka, Hermanus and Dumont d'Urville, and also the *AE* and *Dst* indices, for the moderate and intense geomagnetic storms, respectively, in (a) and (b). In both cases, the geomagnetic storm (magnetically disturbed period) is preceded by a quiet period as can be seen from the *Dst* index. The *AE* index also represents the geomagnetic activity, although restricted to the auroral regions. As can be noted from this figure, the signatures of the geomagnetic disturbances at each station are not identical, although a similar behavior can be identified. These signatures are not similar even for medium and low-latitude stations.

[1]The MLT is obtained from ⟨http://nssdc.gsfc.nasa.gov/space/cgm/cgm.html⟩.

Table 1
Magnetic stations considered in the analysis

Station	Geog. coord.		Geom. coord. (1979)		MLT
	Lat. (°)	Long. (°)	Lat. (°)	Long. (°)	(when UT = 0)
Ft Churchil (FCC)	58.80	265.90	69.83	329.12	6:40
Boulder (BOU)	40.13	254.77	49.32	317.75	7:26
Kakioka (KAK)	36.23	140.18	28.78	210.69	15:06
Hermanus (HER)	−34.42	19.23	−42.02	80.84	23:48
Dumont d'Urville (DRV)	−66.66	140.01	−80.60	235.10	12:53

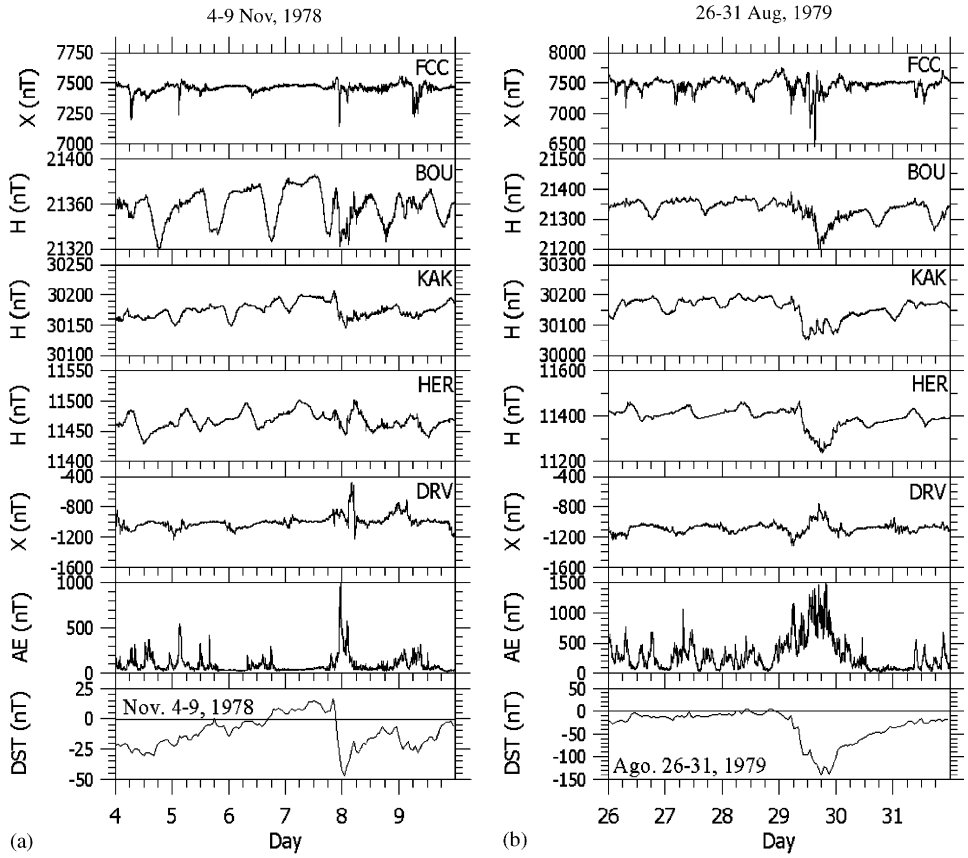

Fig. 3. DST and AE indices and horizontal component magnetograms obtained at DRV, HER, KAK, BOU and FCC for: (a) moderate and (b) intense magnetic storms.

4. Results and discussion

In Fig. 3, the signatures recorded by each magnetic station are quite dissimilar. Some questions arise when analyzing these non-processed data: are there any common features among these magnetograms related to geomagnetic storms? Can any resources offered by the wavelet analysis be explored to elucidate this issue? The idea is to use the wavelet technique to unveil some common features of these signatures.

After the calculation of the wavelet transform, the largest squared amplitudes of the wavelet coefficients at the decomposition levels were analyzed. In all possible decomposition levels, the largest amplitude of the coefficients were related to the geomagnetic disturbances. For each level a cut-off threshold was established.

In this work it was observed that only one decomposition level was able to identify the disturbance; the other two were used just to validate the *shock candidate*

regions. For the chosen wavelet, $\xi_\psi = 0.66667$ and for a sampling rate of 1 min, the pseudo-periods of the first three levels were 3, 6 and 12 min.

Fig. 4 shows the behavior of the square wavelet coefficients for the moderate storm of November 7–8, 1978 at levels $j = 1, 2, 3$, denoted by $d1, d2, d3$. In each panel, from top to bottom, the *Dst* index, the X or H-component of the geomagnetic field and the first three levels of the wavelet coefficients of the discrete wavelet transform (major levels considered for the purpose of this work) are shown. The letters (a)–(e) stand for the stations Fort Churchill, Boulder, Kakioka, Hermanus and Dumont d'Urville, respectively. Taking into account that the highest amplitudes of the wavelet coefficients indicate singularities, in all cases singularity patterns were identified in association with the geomagnetic storm. When the magnetosphere is under quiet conditions (magnetically quiescent periods) the horizontal components of the geomagnetic field recorded in the magnetograms can be represented by smooth functions, and accordingly the wavelet coefficients show very small amplitudes. On the other hand, when a geomagnetic

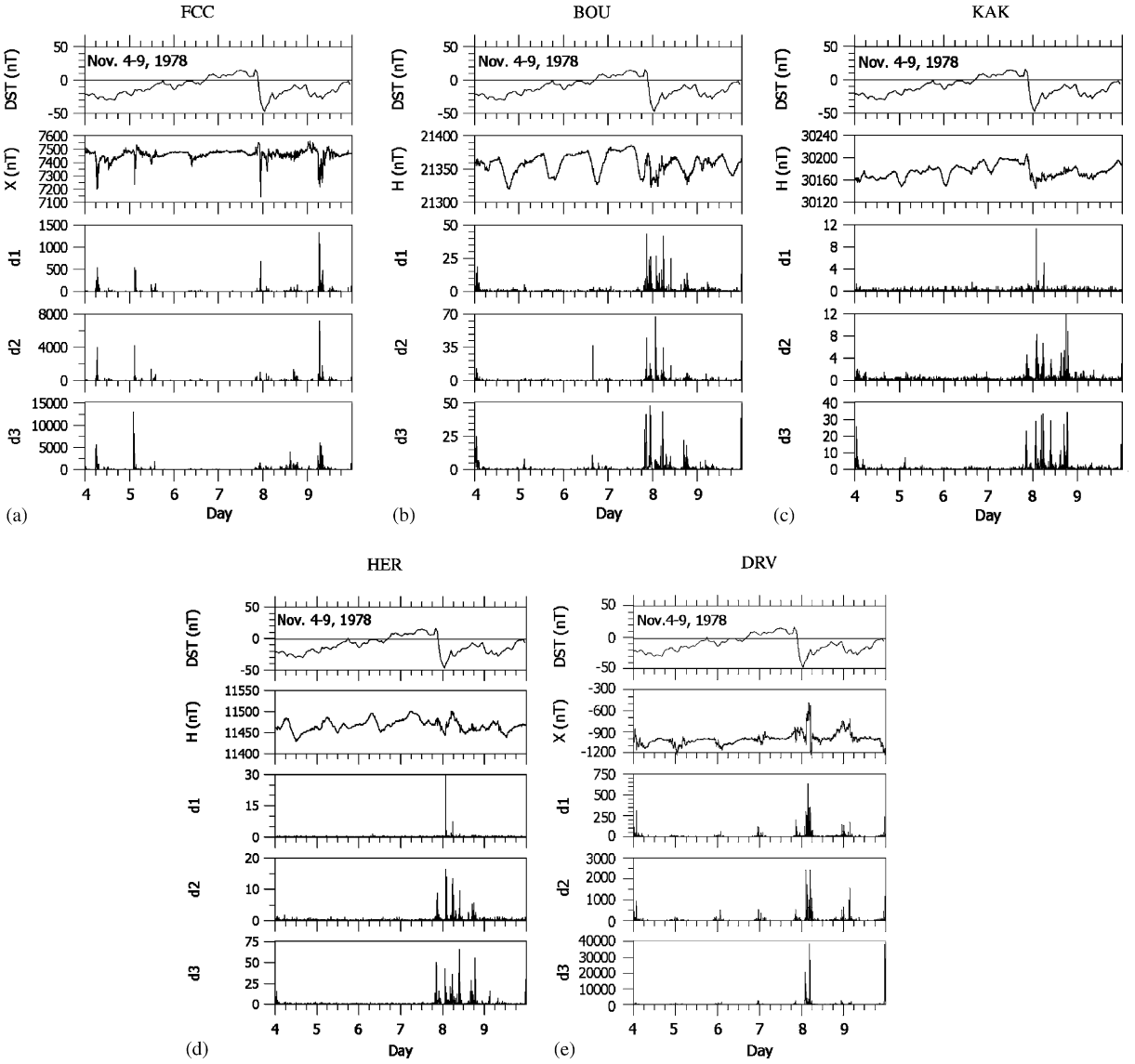

Fig. 4. Geomagnetic field dataset for November 4–9, 1978. The letters (a)–(e) stand for the stations Fort Churchill, Boulder, Kakioka, Hermanus and Dumont d'Urville. Each panel shows from top to bottom, the *Dst* index, the X or H-component of the geomagnetic field and the first three levels of the wavelet coefficients of the discrete wavelet transform.

storm is under development (disturbed periods) the wavelet coefficients are significantly large. These coefficients are able to identify the sudden variations that occur in the geomagnetic field components. These physical effects responsible for these singularities will not be discussed here, since the purpose of this work is simply to characterize the quiescent and non-quiescent periods.

This result can be used as a marker of the geomagnetic activity, an indicator that some process of impulsive energy transfer is going on. A straightforward result of the wavelet technique applied to the dataset is that it allows to distinguish quiescent from non-quiescent periods. The wavelet coefficients of the first decomposition levels of the wavelet transform show indeed a better time localization and then are locally associated with higher frequencies of the geomagnetic disturbance. In the two cases studied, the first three decomposition levels have proved to be sufficient to isolate the singularity patterns. One can observe that the magnetic stations do not show the same singularity pattern in different decomposition levels. This behavior may be related to differences in the magnetic coordinates, type of magnetometer used, local time, ground conductivity and Sq current effects.

Fig. 5 is similar to Fig. 4, but refers to the intense geomagnetic storm of August 29–30, 1979. Also in this case a singularity pattern can be observed for all the magnetograms considered.

In both Figs. 4 and 5, it was possible to identify singularity patterns related to magnetic storm time intervals in the magnetograms of the magnetic stations considered. The highest relative amplitudes of the coefficients are coincident in time, showing that the whole magnetosphere is globally affected, at least in the time resolution considered.

The singularity patterns allowed the identification of quiescent and non-quiescent periods in the horizontal component of the geomagnetic field signals independently of the general signature of the magnetic station considered. Indeed, using this tool, the intrinsic processes of energy transfer are being surveyed.

From the present analysis it seems that for higher latitude magnetic stations (FCC, DRV and BOU), larger amplitude wavelet coefficients are more frequent in the first two decomposition levels, while for lower stations (KAK and HER) the second and the third levels are larger. This fact, actually, confirms the already known concepts that at higher latitudes the penetration of charged particles and the energy injection are characterized by phenomena that involve high-frequency signals, while at lower latitudes coupling processes do exist that attenuate high-frequency signals (Morioka et al., 2003).

Magnetograms obtained at DRV show more transient variations in the decomposition levels of the wavelet transform in the considered time intervals than those obtained at FCC. This is probably due to the fact that the DRV station is at a higher magnetic latitude than the FCC station. Seasonal effects can also play a significant role in the observed signal display. In relation to the lower latitude stations, it was noted that in the three stations used in this analysis (HER, BOU and KAK) the singularities are more clearly seen in the intense magnetic storm during the main phase. This effect is actually the result of a sequence of impulsive energy injections in the ring current system. The small amplitudes observed in the wavelet coefficients for the geomagnetic storm means that the energy transfer process is smooth; while the large amplitudes indicate that there are impulsive energy injections superposed to the smooth background process.

It is already known that variations in the ring current are associated with magnetic field fluctuations on the ground that are depicted by the *Dst* index. On the other hand, these fluctuations are related to energy variations in the ring current, according to the Dessler–Parker–Sckopke theorem (Kivelson and Russell, 1997). Following the *Dst* index for the intense magnetic storm, it can be noted that the magnetic storm begins at about 03 UT on August 29 at 07 UT there is a new injection followed by two others at 10 and at 15 UT (Fig. 3). At 19 UT the *Dst* reaches its minimum value and at 22 UT a second minimum of the same intensity is observed. All these energy injections occur in the main phase and near the double peak minimum. On the other hand, during the moderate magnetic storm new enhancements in the ring current have been noted in the recovery phase: the storm started in November 7 at 23 UT reaching a minimum value 3 h later (Fig. 3). Three new injections occurred at 06, 09, 19 UT, on November 8, and three other occurred on November 9, at 01, 06, 09 UT characterizing a new magnetic storm, still in the recovery phase of the previous one.These new enhancements in the ring current occurring in the main phase of the second storm are clearly identified by the coefficients $d2$ and $d3$ from Kakioka. This result shows that in the recovery phase new energy injections can contribute to enhance the ring current during its symmetrization process, allowing a competition among the physical mechanisms involved. Similar results were reported by Daglis and Kozyra (2002).

It is also worthwhile to mention that in the multiscale analysis of the *AE* index (not shown in this work), a similar behavior has also been detected and other singularities have been found in that signal. In these cases, a poorer temporal localization of the structures was noted in the analyzed signal. The same effect was observed at FCC and DRV and more transients were observed in the latter station.

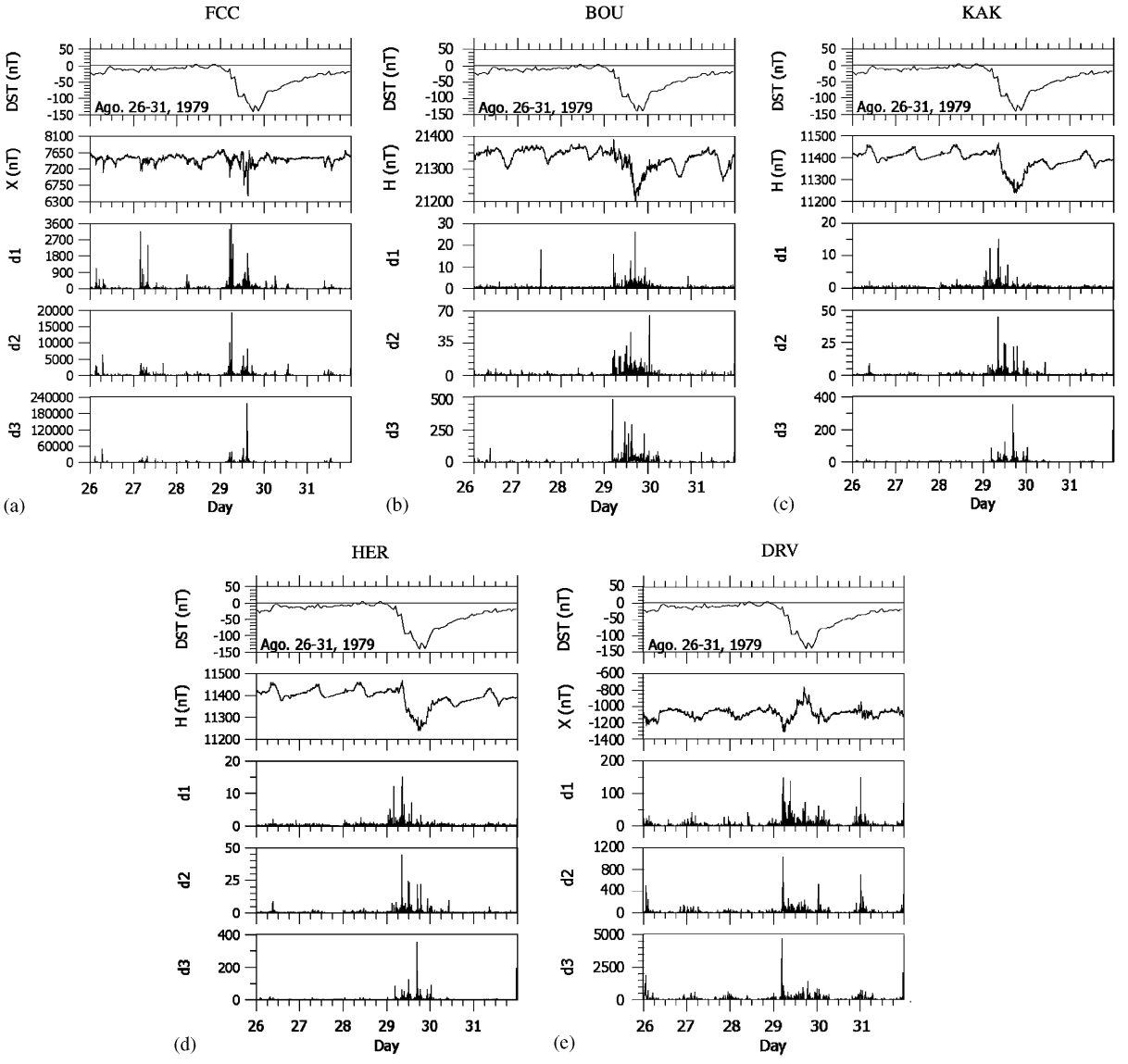

Fig. 5. Geomagnetic field dataset for August 26–31, 1978. The letters (a)–(e) stand for the stations Fort Churchill, Boulder, Kakioka, Hermanus and Dumont d'Urville. Each panel shows from top to bottom, the *Dst* index, the X or H-component of the geomagnetic field and the first three levels of the wavelet coefficients of the discrete wavelet transform.

This may confirm that an injection process in the ring current is associated with an injection process in the auroral region, but the opposite may not be true, what agrees with the physical discussion presented by Tsurutani et al. (1997). It has also been observed that substorms detected at high-latitude stations are not reproduced by singularities at lower latitudes.

A complementary analysis was performed using six latitudinally spaced magnetic stations from North to South[2] for a more recent magnetic storm (May 14–17, 1997). The resulting decomposition levels showed a behavior quite similar to those described here.

[2]Station name and geomagnetic coordinates: Tixie Bay (60.99°; −167.19°); Kanoya (21.12°; −160.15°); Guam (4.57°; −145.24°); Canberra (−43.34°; −135.51°); Kakadu (−22.75°; −155.18°) and Dumont d 'Urville (−75.07°; −127.83°) from ⟨http://swdcwww.kugikyoto-u.ac.jp/catmap/tmp/B901lst.txt⟩.

5. Conclusions

The study of geomagnetic storms still remains an important issue, that is far from being fully understood. To date, the most common index to quantify the development of geomagnetic storms is the *Dst* index, that is based on a post-processed calculation using only four magnetometers.

This work has intended to work out raw magnetometer data using the Daubechies orthogonal wavelet analysis in order to identify *shocks* (singularities) in the datasets.

The highest wavelet coefficient amplitudes of the first three decomposition levels were able to identify the common singularities among the magnetograms selected.

This analysis has shown that:

- The maximum amplitudes of the wavelet coefficients can be used to identify non-quiescent from quiescent periods.
- The resulting singularity patterns were coincident with the main phase of the geomagnetic storms.
- The small amplitudes observed in the wavelet coefficients mean that the energy transfer process is smooth, while the large amplitudes indicate that there are impulsive energy injections superposed to the smooth background process.

Based on its ability to provide an objective analysis, the wavelet technique has revealed a helpful tool in the study of magnetospheric phenomena such as the time localization of geomagnetic storms.

Acknowledgements

The authors wish to thank CNPq for the Grants 478707/2003-7, 477819/2003-6, 382465/01-6 and SPIDR-Boulder and WDC-Kyoto for the datasets used in this work.

References

Abry, P., 1997. Ondelettes et turbulences - multirésolutions, algorithmes de décompositions, invariance d'échelle et signaux de pression. Diderot, Editeurs des sciences et des arts, Paris.

Baker, D.N., 1998. What is space weather? Advances in Space Research 22, 7–16.

Bayer, M., Freeden, W., Maier, T., 2001. A vector wavelet approach to iono- and magnetospheric geomagnetic satellite data. Journal of Atmospheric and Solar-Terrestrial Physics 63 (6), 581–597.

Chui, C., 1992a. An Introduction to Wavelets, vol. 1. Academic Press, New York.

Chui, C. (Ed.), 1992b. Wavelets: A Tutorial in Theory and Applications, vol. 2. Academic Press, New York.

Clúa de Gonzalez, A.L., Mendes da Costa, A., Gonzales, W.D., 2004. Ring current space–time inhomogeneities in intense geomagnetic storms. Geofisica Internacional 43 (2), 205–215.

Daglis, I.A., Kozyra, J.U., 2002. Outstanding issues of ring current dynamics. Journal of Atmospheric and Solar-Terrestrial Physics 64 (2), 253–264.

Daubechies, I., 1992. Ten Lectures on Wavelets, CBMS-NSF Regional Conference (Series in Applied Mathematics), vol. 61. SIAM, Philadelphia, PA.

Domingues, M.O., Mendes, O.J., Mendes da Costa, A., 2005. Wavelet techniques in atmospheric sciences. Advances in Space Research 35 (5), 831–842.

Foufoula-Georgiou, E.K., Kumar, P. (Eds.), 1995. Wavelet in Geophysics. Academic Press, New York, 373pp.

Gonzalez, W.D., Joselyn, J.A., Kamide, Y., Kroehl, H.W., Rostoker, G., Tsurutani, B.T., Vasyliunas, V.M., 1994. What is a geomagnetic storm? Journal of Geophysical Research 99 (A4), 5771–5792.

Iyemori, T., Araki, T., Kamei, T., Takeda, M., 1998. Mid-latitude geomagnetic indices asy and sym 1997. Data Analysis Center for Geomagnetism and Space Magnetism, Kyoto University, Japan, (Number 8).

Jankovicová, D., Dolinský, P., Valach, F., Vörös, Z., 2002. Neural network-based nonlinear prediction of magnetic storms. Journal of Atmospheric and Solar-Terrestrial Physics 64 (5–6), 651–656.

Jawerth, B., Sweldens, W., 1994. An overview of wavelet based multiresolution analyses. SIAM Review 36 (3), 377–412.

Kamide, Y., Baumjohann, W., Daglis, I.A., Gonzalez, W.D., Grande, M., Joselyn, J.A., McPherron, R.L., Phillips, J.L., Reeves, E.G.D., Rostoker, G., Sharma, A.S., Singer, H.J., Tsurutani, B., Vasyliunas, V.M., 1998. Current understanding of magnetic storms: storm/substorm relationships. Journal of Geophysical Research 103 (A8), 17705–17728.

Kivelson, M.G., Russell, C.T., 1997. Introduction to Space Physics. Cambridge University Press, Cambridge.

Mallat, S., 1991. Multiresolution approximations and wavelets orthonormal bases. Transaction of American Mathematical Society 315, 334–351.

Mayaud, P.N., 1980. Derivation, meaning, and use of geomagnetic indices. Geophysical Monograph, vol. 22. American Geophysical Union, Washington, DC.

Mendes, O.J., Gonzalez, W.D., Clúa de Gonzalez, A.L., Pinto, O.J., Tsurutani, B.T., 1994. Solar wind-magnetosphere coupling during moderate geomagnetic storms (1978–1979). In: Solar Terrestrial Energy Program, vol. 5. COSPAR, New York, pp. 297–300.

Meyer, Y., 1990. Ondelettes et Operateurs. Hermann, Paris.

Morioka, A., Miyoshi, Y., Seki, T., Tsuchiya, F., Misawa, H., Oya, H., Matsumoto, H., Hashimoto, K., Mukai, T., Yumoto, K., Nagatsuma, T., 2003. AKR disappearance during magnetic storms. Journal of Geophysical Research 108 (A6), 1226–1235.

O'Brien, T., McPherron, R.L., 2000. Forecasting the ring current index dst in real time. Journal of Atmospheric and Solar-Terrestrial Physics 62 (14), 1295–1299.

Ruskai, M.B., Beylkin, G., Coifman, R., Daubechies, I., Mallat, S. Meyer, Y., Raphael, L. (Eds.), 1992. Wavelets and their Applications. Jones and Bartlett, Boston, MA.

SPIDR, 2004. ⟨http://spidr.ngdc.noaa.gov/spidr⟩.

Strang, G., Nguyen, T., 1996. Wavelet and Filters Bank. Wellesley-Cambridge, Cambridge.

Sugiura, M., Kamei, T., 1991. Equatorial dst Index 1957–1986. ISGI Publications Office.

Takahashi, S., Iyemori, T., Takeda, M., 1990. Ring current response to impulsive southward imf: a cause of second development of the dst index. Journal Geomagnetism Geoelectricity 42, 1325–1331.

Tsunomura, S., 1998. Characteristics of geomagnetic sudden commencement observed in middle and low latitudes. Earth Planets Space 50 (9), 755–772.

Tsurutani, B.T., Gonzalez, W.D., Tang, F., Akasofu, S.I., Smith, E.J., 1988. Origin of interplanetary southward magnetic fields responsible for major magnetic storms near solar maximum (1978–1979). Journal of Geophysical Research 93 (A8), 8519–8531.

Tsurutani, B.T., Gonzalez, W.D., Kamide, Y., Arballo, J.K. (Eds.), 1997. The role of substorms in generation of magnetic storms. In: Magnetic Storms. Geophysical Monograph, vol. 98. American Geophysical Union, Washington.

Valdivia, J.A., Vassiliadis, D., Klimas, A., 1999. Spatiotemporal activity of magnetic storms. Journal of Geophysical Research 104 (6), 12239–12250.

WDC, 2004. ⟨http://swdcwww.kugi.kyoto-u.ac.jp/index.html⟩.